Disentangled Control of Multi-Agent Systems

Ruoyu Lin¹, Gennaro Notomista², and Magnus Egerstedt¹

Abstract—This paper develops a general framework for multiagent control synthesis, which applies to a wide range of problems with convergence guarantees, regardless of the complexity of the underlying graph topology and the explicit time dependence of the objective function. The proposed framework systematically addresses a particularly challenging problem in multi-agent systems, i.e., decentralization of entangled dynamics among different agents, and it naturally supports multi-objective robotics and real-time implementations. To demonstrate its generality and effectiveness, the framework is implemented across three experiments, namely time-varying leader-follower formation control, decentralized coverage control for time-varying density functions without any approximations, which is a long-standing open problem, and safe formation navigation in dense environments.

Index Terms—Disentangled control, networks of autonomous agents, distributed algorithms/control, robotics.

I. Introduction

Multi-agent systems are increasingly used to tackle problems across energy networks, transportation systems, robotics, reinforcement learning, and generative modeling (see, e.g., [1]–[9]). Their strength lies in shaping interactions and distributing decision making, policy synthesis, or action generation among autonomous agents, enabling effective collaboration, adaptivity to changing environments, and resilience to individual failures. At the heart of these capabilities is decentralization, which also helps ensure scalability by avoiding a prohibitive increase in per-agent computational load as the number of agents grows.

While multi-agent systems have been adopted in a wide variety of applications, many theoretical developments have been informed by ideas from multi-agent control, through canonical problems such as formation control [10], coverage control [11], caging control [12], containment control [13], and consensus control (e.g., rendezvous, flocking, and cyclic pursuit) [14]. Although these problems differ in their specific objectives, they share common underlying structures such as local interaction rules and coherent system-level behaviors. This observation leads to the question: Can one develop a general framework that captures these diverse tasks within a unified formulation? Such a framework may not only advance a new understanding of decentralized multi-agent control, but also inspire extensions to other fields.

This work was supported in part by the U.S. Army Research Lab through ARL DCIST CRA W911NF-17-2-0181, and in part by the NSERC Discovery under Grant RGPIN-2023-03703.

¹Ruoyu Lin and Magnus Egerstedt are with the Department of Electrical Engineering and Computer Science, University of California, Irvine, CA 92697, USA. Email: {rlin10, magnus}@uci.edu

²Gennaro Notomista is with the Department of Electrical and Computer Engineering, University of Waterloo, Waterloo, ON, Canada. Email: gennaro.notomista@uwaterloo.ca

The gradient flow method has been explored as a general framework for multi-agent control (see, e.g., [2], [14]), achieving decentralization under certain graph topologies with convergence guarantees by leveraging LaSalle's invariance principle. However, such guarantees do not necessarily hold in time-varying settings, which will be explored in Section III. Similarly, a constraint-driven method developed in [15] provides a general framework for multi-agent control. However, there are several pieces not covered in [15], especially when the underlying graph exhibits complicated topologies or the objective functions become time-varying, which will be discussed in detail in Appendix A.

Another challenge arises from certain forms of dynamics interdependency in multi-agent systems. Specifically, rather than acting based on its own state and those of its neighbors, each agent cannot make its decisions or determine its actions without explicitly knowing those of its neighbors, while these neighbors face the same dilemma simultaneously (see, e.g., [16]-[21]). Existing work has sought to address this type of challenge through approaches such as modeling neighbor dynamics as bounded disturbance within a robust control framework [16], [17], zero-order-hold approximation of neighbor dynamics [18], centralized aggregation followed by decentralized approximation [19], and iterative negotiation toward a coherent solution [20], [21]. Although these methods have enabled practical advances, their applicability often involves trade-offs among performance conservatism, local communication requirements, computational complexity, and provable convergence guarantees. An exact decentralization mechanism without reliance on simplifying approximations or communication with neighbors has remained elusive.

In this paper, we aim to develop a general multi-agent control framework, which can address the following three independent challenges, all while preserving convergence guarantees without relying on any simplifying approximations:

- enabling decentralized control synthesis,
- handling time-varying objective functions, and
- accommodating arbitrary underlying graph topologies (i.e., undirected graph, directed graph, mixed graph, or piecewise-constant graph).

The main contributions of this paper are summarized as follows.

- (1) We provide new insights into [15], [22], and maintain terminological consistency by identifying a special case in which the time-varying control barrier function provides the same functionality as the time-varying control Lyapunov function.
- (2) We adapt the nonsmooth control Lyapunov function framework in [23] to the time-varying case, which can

be used to handle piecewise-constant graph topologies in multi-agent systems, where the edges can appear or disappear at finitely many instants over a finite time interval.

- (3) We identify two classes of challenges in decentralized control synthesis in multi-agent systems, and develop Lyapunov-based theorems that resolve them and guarantee convergence. We then introduce an optimization framework that can integrate both theories as it accommodates multi-objective optimization. This framework addresses all the three challenges presented above, supports real-time computation, and is suitable for solving a broad range of multi-agent problems in real-world systems.
- (4) The generality and effectiveness of the proposed framework are demonstrated through one simulation and two physical experiments, namely time-varying leader-follower formation control, decentralized coverage control for time-varying density functions, and safe formation navigation in an environment with densely distributed obstacles. Notably, the problem of decentralized coverage control for time-varying densities without any approximations has remained a long-standing challenge for which, to the best of our knowledge, no convergence guarantee has been established over the past two decades (even when disregarding the treatment of the underlying piecewise-constant graph topology).

This paper proceeds as follows. In Section II, we present necessary definitions used throughout this paper. In Section III, first, we identify a situation where the time-varying control barrier and control Lyapunov functions have the same functionality, which helps terminological consistency when we highlight new insights into [15], [22] in Appendix A. Then, we extend the nonsmooth control Lyapunov function framework in [23] to the time-varying case for the preparation of dealing with piecewise-constant graph topologies. In Section IV, we identify two types of Lyapunov functions that cause key challenges in decentralized multi-agent control and develop theorems to address them respectively, followed by a general optimization framework, whose effectiveness is demonstrated across three experiments in Section V. Finally, Section VI concludes the paper.

II. PRELIMINARIES

Given a vector field $X: \mathbb{R}^n \times \mathbb{R}_{\geq 0} \to \mathbb{R}^n$, a set of initial states $\mathcal{A} \subset \mathbb{R}^n$, and a time interval $\mathcal{I} \subseteq \mathbb{R}_{\geq 0}$, the flow generated by X is defined as the map $\Phi_X: \mathcal{A} \times \mathcal{I} \to \mathbb{R}^n$, e.g., [24]–[26], satisfying $\Phi_X(x,0) = x$ and

$$\frac{\partial}{\partial t} \Phi_X(x,t) = X(\Phi_X(x,t),t). \tag{1}$$

Fixing an initial state $x_0 = \Phi_X(x_0, 0) \in \mathcal{A}$, (1) becomes $\frac{d}{dt}\Phi_X(x_0, t) = X(\Phi_X(x_0, t), t)$, which is equivalent to

$$\frac{d}{dt}x(t) = X(x(t), t), \quad x(0) = x_0,$$
 (2)

whose solution $x(t) = \Phi_X(x_0, t)$ is called a trajectory (or integral curve, e.g., [25]). Such x(t) exists and is unique for each $x_0 \in \mathcal{A}$ on a maximal interval $[0, \tau_{\max}(x_0))$, if

the time-varying¹ vector field X(x,t) is continuous in time t and is locally Lipschitz in state x uniformly on compact time intervals (see, e.g., [26]–[28]). Throughout this paper, we further assume that the dynamical system of interest in the form of (2) (equivalently, the corresponding vector field X(x,t)) is forward complete, i.e., $\tau_{\max}(x_0) = \infty, \ \forall x_0 \in \mathcal{A}$, so the solution $\Phi_X(x_0,t)$ is well-defined $\forall t \geq 0, \ \forall x_0 \in \mathcal{A}$.

For a real-valued function $F: \mathbb{R}^n \times \mathbb{R}_{\geq 0} \to \mathbb{R}$ of class C^1 in x and t, the total derivative (or Lagrangian derivative) of F along a trajectory $x(t) = \Phi_X(x_0, t)$ of (2) is the sum of the Lie derivative and the Eulerian derivative (see, e.g., [29]), i.e.,

$$\frac{d}{dt}F(x(t),t) = L_X F(x(t),t) + \frac{\partial}{\partial t}F(x(t),t), \quad (3)$$

where the Lie derivative is calculated as

$$L_X F(x,t) = \nabla_x F(x,t) X(x,t),$$

in which the gradient of F with respect to x is defined as

$$\nabla_x F := \frac{\partial}{\partial x} F \in \mathbb{R}^{1 \times n},$$

which takes the row vector convention. To distinguish the Jacobian notation from the gradient notation, for a vector-valued function $G: \mathbb{R}^n \times \mathbb{R}_{\geq 0} \to \mathbb{R}^p$, we denote its Jacobian with respect to x by $\frac{\partial G}{\partial x} \in \mathbb{R}^{p \times n}$. Throughout this paper, for notational compactness, we sometimes also use the dot notation (\cdot) to represent the total time derivative of a quantity.

If $F: \mathbb{R}^n \times \mathbb{R}_{\geq 0} \to \mathbb{R}$ is locally Lipschitz in x and C^1 in t, the Clarke generalized gradient [30] is defined as

$$\partial_x^{\circ} F(x,t) := \operatorname{co} \left\{ \lim_{k \to \infty} \nabla_x F(\tilde{x}_k, t) \,\middle|\, \tilde{x}_k \to x, \, \tilde{x}_k \notin \mathcal{E}_t \right\},$$

in which co denotes the convex hull of a set, and \mathcal{E}_t of Lebesgue measure zero is the set where F is nondifferentiable with respect to x at time t. Correspondingly, the nonsmooth² Lie derivative, e.g., [31], [32], is calculated as

$$L_X^{\circ}F(x,t) = \sup_{\nu \in \partial_x^{\circ}F(x,t)} \nu X(x,t).$$

Given a continuous function $\eta: \mathbb{R}_{\geq 0} \to \mathbb{R}$, the Dini derivative, e.g., [28], is defined as

$$D_t^+ \eta(t) \coloneqq \limsup_{\delta t \downarrow 0} \frac{\eta(t + \delta t) - \eta(t)}{\delta t}.$$

The above definitions and notations will be used throughout the subsequent theoretical analysis.

III. CONTROL LYAPUNOV FUNCTIONS

Given a control-affine system,

$$\dot{x}(t) = f(x(t)) + g(x(t)) u(x(t), t), \tag{4}$$

the controller $u: \mathbb{R}^n \times \mathbb{R}_{\geq 0} \to \mathcal{U} \subset \mathbb{R}^m$, where \mathcal{U} is a nonempty compact set of admissible control inputs, together with the vector fields $f: \mathbb{R}^n \to \mathbb{R}^n$ and $g: \mathbb{R}^n \to \mathbb{R}^{n \times m}$,

 $^{^{1}}$ In this paper, the adjective *time-varying* is reserved for quantities that depend explicitly on both x and t.

 $^{^2}$ In this paper, the term *nonsmooth* is used to refer to functions that are not of class C^1 (i.e., not continuously differentiable), following the terminology convention of [31].

determines the vector field $X(x,t)=f(x)+g(x)\,u(x,t)$. Throughout this paper, for each initial state x_0 , there exists a unique maximal trajectory $x(t)=\Phi_{f+gu}(x_0,t)$, as we assume f(x),g(x) are locally Lipschitz in x, and u(x,t) is continuous in t and is locally Lipschitz in x uniformly on compact time intervals (see, e.g., [25]–[27]). In addition, f,g are given a priori while u is designed to induce the flow Φ_{f+gu} , and we only consider controllers u for which the closed-loop vector field f+gu is forward complete.

Consider the objective of minimizing a function $J: \mathbb{R}^n \to \mathbb{R}$ of class C^1 . It can be asymptotically achieved by following along the trajectory obtained from the gradient flow such that

$$\dot{x}(t) = -\nabla_x J(x(t))^{\top},\tag{5}$$

as $\frac{d}{dt}J(x(t)) = \nabla_x J(x(t))\dot{x}(t) = -\|\nabla_x J(x(t))\|^2 \le 0$. The gradient flow method can be viewed as the continuous-time version of the gradient descent method (see, e.g., [33], [34]).

However, when the cost (or objective) function becomes time-varying, i.e., $J:\mathbb{R}^n\times\mathbb{R}_{\geq 0}\to\mathbb{R}_{\geq 0}$, the gradient flow method does not necessarily guarantee its convergence. This is because the Eulerian derivative, as seen in (3), can also contribute to the total rate of change of J(x(t),t). To address this challenge, one can resort to the time-varying control Lyapunov function (TV-CLF) reviewed below (see, e.g., [35] for earlier work on CLFs for time-varying systems), which provides a systematic way of ensuring convergence of time-varying cost functions through feedback controllers.

Definition III.1. (Definition 5.1 in [18]) A class C^1 function $V: \mathbb{R}^n \times \mathbb{R}_{\geq 0} \to \mathbb{R}_{\geq 0}$ is a TV-CLF with respect to (4) if there exists a locally Lipschitz class K function $\alpha: [0, a) \to \mathbb{R}_{\geq 0}$ with $a < \infty$ such that

$$\inf_{u \in \mathcal{U}} \left(L_X V(x,t) + \frac{\partial}{\partial t} V(x,t) + \alpha(V(x,t)) \right) \leq 0,$$

 $\forall x \in \mathbb{R}^n \text{ such that } V(x,t) < a, \ \forall t \geq 0.$

Lemma III.1. (Lemma 5.2 in [18]) If V(x,t) is a TV-CLF and $V(x(0),0) < a < \infty$ per Definition III.1, then $\lim_{t\to\infty}V(x(t),t)=0$ along the trajectory $x(t)=\Phi_{f+gu}(x(0),t)$ under any time-varying state-feedback controller u(x,t) such that $L_XV(x(t),t)+\frac{\partial}{\partial t}V(x(t),t)+\alpha(V(x(t),t))\leq 0, \ \forall t\geq 0.$

Proof. See [18] following [28].
$$\Box$$

For consistency in terminology in Appendix A presenting new insights into [15], [22], we observe that the TV-CLF and the time-varying control barrier function (TV-CBF) have the same functionality in a special case.

First, we revisit the TV-CBF as follows. Consider a timevarying set, its boundary, and its interior given by

$$\mathcal{C}(t) = \{ x \in \mathbb{R}^n \mid h(x,t) \ge 0 \},$$

$$\partial \mathcal{C}(t) = \{ x \in \mathbb{R}^n \mid h(x,t) = 0 \},$$

$$\mathcal{C}^{\circ}(t) = \{ x \in \mathbb{R}^n \mid h(x,t) > 0 \},$$
(6)

respectively, where $h \in C^1 : \mathbb{R}^n \times \mathbb{R}_{\geq 0} \to \mathbb{R}$, and $\nabla_x h(x,t) \neq 0$, $\forall x \in \partial \mathcal{C}$, $\forall t \geq 0$.

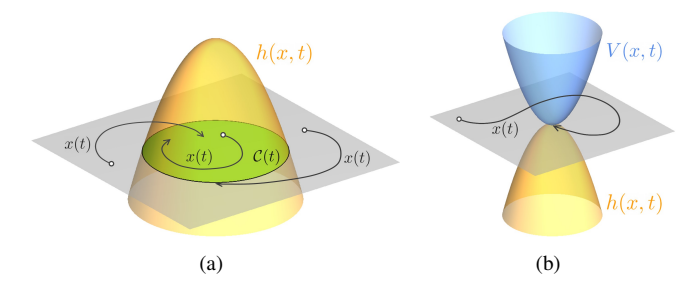


Figure 1. (a) Illustration of the attractivity of TV-CBF; (b) Illustration of a special case of TV-CBF which has the same functionality as TV-CLF, where $\mathcal{C}(t) = \{x \in \mathbb{R}^n \mid V(x,t) = 0\}, \ \forall t \geq 0.$

Definition III.2. (Definition 4 in [36] following [37], [38]) A class C^1 function h(x,t) defining (6) is a TV-CBF with respect to (4) and (6) if there exists a locally Lipschitz extended class \mathcal{K}_{∞} function $\gamma: \mathbb{R} \to \mathbb{R}$ such that

$$\sup_{u \in \mathcal{U}} \left(L_X h(x,t) + \frac{\partial}{\partial t} h(x,t) + \gamma(h(x,t)) \right) \ge 0,$$

 $\forall x \in \mathbb{R}^n, \ \forall t \geq 0.$

Lemma III.2. (Theorem 2.1 in [39]) If h(x,t) is a TV-CBF per Definition III.2, then C(t) is rendered attractive, by any time-varying state-feedback controller u(x,t) such that $L_Xh(x(t),t)+\frac{\partial}{\partial t}h(x(t),t)+\gamma(h(x(t),t))\geq 0, \ \forall t\geq 0, \ in$ the sense that

$$x(0) \in \mathcal{C}(0) \Rightarrow x(t) \in \mathcal{C}(t), \forall t \ge 0$$
 (7)

$$x(0) \notin \mathcal{C}(0) \Rightarrow x(t) \to \in \partial \mathcal{C}(t) \text{ as } t \to \infty$$
 (8)

or

$$\exists \tau > 0, \text{ s.t. } x(t) \in \mathcal{C}(t), \forall t \geq \tau, \quad (9)$$

where (9) includes two specific cases: (a) $\exists \tau > 0$ such that $x(t) \in \partial \mathcal{C}(t)$, $\forall t \geq \tau$; or (b) $\exists \tau > 0$ such that $x(\tau) \in \partial \mathcal{C}(\tau)$ and $x(t) \in \mathcal{C}^{\circ}(t)$, $\forall t > \tau$, as illustrated in Fig. 1(a).

Note that whether (8) or (9) will occur depends on the specific property of γ . Likewise, in terms of the TV-CLF, whether asymptotic convergence or finite-time convergence will occur depends on the property of α .

Remark III.1. According to Lemma III.1 and Lemma III.2, in the special case when $V(x,t) = -h(x,t) \ge 0$, $\forall x \in \mathbb{R}^n$, $\forall t \ge 0$, such TV-CBF h(x,t) and TV-CLF V(x,t) have the same functionality, as illustrated in Fig. 1(b).

The problem of minimizing J(x,t) seems to be solved by Lemma III.1. However, its decentralized realization in multiagent systems is nontrivial in general, which is the main focus of this papaer. One key problem arises from sudden changes of the underlying graph topology, i.e., edges defining adjacency can suddenly appear or disappear (with a finite number of switching instants within a finite time interval). In preparation for the next section where we address this problem, we adapt the nonsmooth CLF framework in [23] (see, e.g., [40] for earlier work on nonsmooth CLFs) to the time-varying case.

Lemma III.3. (Comparison lemma [28]) Consider the scalar differential equation $\dot{z}(t) = \phi(z(t),t)$ with $z(0) = z_0$, where $\phi(z,t)$ is locally Lipschitz in z and continuous in t. Let y(t) be a continuous function whose Dini derivative $D_t^+y(t)$ satisfies the differential inequality

$$D_t^+ y(t) \le \phi(y(t), t), \quad y(0) \le z_0, \quad \forall t \ge 0,$$

assuming forward completeness, then

$$y(t) \le z(t), \quad \forall t \ge 0.$$

Proof. See [28].

Definition III.3. (Nonsmooth TV-CLF) A continuous function $V: \mathbb{R}^n \times \mathbb{R}_{\geq 0} \to \mathbb{R}_{\geq 0}$ is a nonsmooth TV-CLF (NS-TV-CLF) with respect to (4) if V(x,t) is locally Lipschitz in x and C^1 in t, and there exists a locally Lipschitz class K function $\alpha: [0,a) \to \mathbb{R}_{\geq 0}$ with $a < \infty$ such that

$$\inf_{u \in \mathcal{U}} \left(L_X^{\circ} V(x,t) + \frac{\partial}{\partial t} V(x,t) + \alpha(V(x,t)) \right) \le 0,$$

 $\forall x \in \mathbb{R}^n \text{ such that } V(x,t) < a, \ \forall t \geq 0.$

Theorem III.1. If V(x,t) is a NS-TV-CLF and $V(x(0),0) < a < \infty$ per Definition III.3, then $\lim_{t\to\infty} V(x(t),t) = 0$ along the trajectory $x(t) = \Phi_{f+gu}(x(0),t)$ under any time-varying state-feedback controller u(x,t) such that $L_X^\circ V(x(t),t) + \frac{\partial}{\partial t} V(x(t),t) + \alpha(V(x(t),t)) \leq 0, \ \forall t \geq 0.$

Proof. According to [31], [32], we have

$$D_t^+V\big(x(t),t\big) \leq L_X^{\circ}V\big(x(t),t\big) + \frac{\partial}{\partial t}V\big(x(t),t\big), \quad \forall t \geq 0.$$

Hence, we obtain

$$D_t^+V(x(t),t) < -\alpha(V(x(t),t)), \quad \forall t > 0.$$

Consider a reference function \bar{V} satisfying the scalar differential equation

$$\dot{\bar{V}}(t) + \alpha(\bar{V}(t)) = 0, \quad \bar{V}(0) = V(x(0), 0),$$
 (10)

where $\alpha:[0,a)\to\mathbb{R}_{\geq 0}$ with $a<\infty$ is a locally Lipschitz class $\mathcal K$ function. Then, per Lemma 4.4 of [28], for any 0< V(x(0),0)< a, (10) has a unique solution $\bar V(t),\ \forall t\geq 0$ (assuming forward completeness), and

$$\bar{V}(t) = \bar{\alpha}(V(x(0), 0), t),$$

where $\bar{\alpha}:[0,a)\times\mathbb{R}_{\geq 0}\to\mathbb{R}_{\geq 0}$ is a class \mathcal{KL} function. By Lemma III.3, we obtain

$$V(x(t), t) \le \bar{\alpha}(V(x(0), 0), t), \quad \forall t \ge 0.$$

Since $\bar{\alpha}$ is a class \mathcal{KL} function, we have

$$\lim_{t \to \infty} \bar{\alpha}(V(x(0), 0), t) = 0,$$

resulting in
$$\lim_{t\to\infty} V(x(t),t)=0$$
.

Theorem III.1 is a more general version of Lemma III.1. For a multi-agent task, if the underlying graph topology stays constant, then Theorem III.1 degenerates to Lemma III.1.

Another challenge, as discussed in Section I, arises from certain forms of dynamics interdependency in multi-agent systems, which will be explored in the following content by using the theoretical tools presented in this section.

IV. DISENTANGLED CONTROL

Consider a system of N agents, each of whose states of interest is denoted by $x_i \in \mathbb{R}^{n_i}, \, \forall i \in \mathcal{N} \coloneqq \{1,\dots,N\}$. The vector $x = [x_1^\top,\dots,x_N^\top]^\top \in \mathbb{R}^{\sum_{i \in \mathcal{N}} n_i}$ consists of the states of all N agents. Each agent is governed by the control-affine dynamics

$$\dot{x}_i(t) = f_i(x_i(t)) + g_i(x_i(t)) u_i, \quad \forall i \in \mathcal{N}, \tag{11}$$

where the vector fields $f_i : \mathbb{R}^{n_i} \to \mathbb{R}^{n_i}$, $g_i : \mathbb{R}^{n_i} \to \mathbb{R}^{n_i \times m_i}$, and the controller $u_i \in \mathcal{U}_i \subset \mathbb{R}^{m_i}$ determine the time-varying vector field $X_i(x_i,t) = f_i(x_i) + g_i(x_i) u_i$ and satisfy the same assumptions as those imposed in (4).

Theorem III.1 provides a systematic way toward convergence-guaranteed time-varying controller synthesis, and it can be directly leveraged by stacking all agents' states and carrying out a centralized synthesis. However, the centralized approach, as discussed in Section I, is not an ideal architecture for multi-agent settings. For a multi-agent task, if the objective is to minimize $J(x,t) = \sum_{i \in \mathcal{N}} J_i(x_i,t)$ and the cost function for each agent $J_i : \mathbb{R}^{n_i} \times \mathbb{R}_{\geq 0} \to \mathbb{R}_{\geq 0}$ depends only on x_i and t, then it can be achieved in a decentralized manner by directly applying Theorem III.1 to each agent.

However, when the cost function for each agent also depends on the states of other agents or when multiple agents share a single cost function that depends on their states, decentralized control synthesis for each agent becomes nontrivial. This is because the total derivatives of these types of cost functions involve the dynamics of multiple agents simultaneously, which typically requires centralized control synthesis for all the agents involved. We refer to such dynamics as *entangled* dynamics in multi-agent systems. By *entangled* we mean that in order for an agent to synthesize its controller, it must have access to the controllers of certain other agents, and in turn, those agents require this agent's controller (and possibly the controllers of additional agents) to complete their own control synthesis. This creates a more complicated version of the "chicken-and-egg" coupling issue.

Against this backdrop, developing a decentralized framework where u_i in (11) can be specifically synthesized as $u_i: \mathbb{R}^{\sum_{i \in \mathcal{N}} n_i} \times \mathbb{R}_{\geq 0} \to \mathcal{U}_i \subset \mathbb{R}^{m_i}$ that does not depend on $u_j \in \mathcal{U}_j \subset \mathbb{R}^{m_j}$, for any $j \in \mathcal{N} \setminus \{i\}$, becomes the focus of our investigation in this section. To this end, we identify two different types of entangled TV-CLFs, which constitute the main obstacles to directly applying Theorem III.1 to multiagent systems in a decentralized manner. Correspondingly, we develop Lyapunov-based theorems ensuring convergence guarantees to address these two cases.

Definition IV.1. For an $\mathcal{N}^{\mathrm{SE}} \in \mathcal{S}^{\mathrm{SE}} \subseteq 2^{\mathcal{N}} \setminus \{\varnothing\}$, where $2^{\mathcal{N}}$ denotes the power set of \mathcal{N} , let $\mathcal{N}_i^{\mathrm{SE}} = \mathcal{N}^{\mathrm{SE}} \setminus \{i\}$ denote the neighbor set of Agent i in the Shared-Entangled graph (SE graph) $\mathcal{G}^{\mathrm{SE}} = (\mathcal{N}^{\mathrm{SE}}, \mathcal{E}^{\mathrm{SE}})$, which is a complete graph. An NS-TV-CLF

$$V_{\mathcal{N}^{\text{SE}}}: \mathbb{R}^{\sum_{i \in \mathcal{N}^{\text{SE}}} n_i} \times \mathbb{R}_{>0} \to \mathbb{R}_{>0}$$
 (12)

is called a Shared-Entangled NS-TV-CLF (SE-NS-TV-CLF) if it depends only on $\{x_i\}_{i\in\mathcal{N}^{\mathrm{SE}}}$ and t.

Intuitively, the SE-NS-TV-CLFs arise in scenarios where there exist groupwise shared objectives. For this type of CLFs, inspired by the idea of [41], we propose the following theorem to achieve the decentralized realization of Theorem III.1 in multi-agent systems.

Theorem IV.1. (Constraint Allocation) For any \mathcal{N}^{SE} per Definition IV.1, if each agent is executing the time-varying state-feedback controller $u_i(\{x_i\}_{i\in\mathcal{N}^{SE}},t)$ such that

$$\sup_{\zeta_{i} \in \partial_{x_{i}}^{\circ} V_{\mathcal{N}^{SE}}} \zeta_{i} \dot{x}_{i} + w_{\mathcal{N}^{SE}}^{i} \left(\frac{\partial}{\partial t} V_{\mathcal{N}^{SE}} (\{x_{i}\}_{i \in \mathcal{N}^{SE}}, t) \right) + \alpha \left(V_{\mathcal{N}^{SE}} (\{x_{i}\}_{i \in \mathcal{N}^{SE}}, t) \right) \right) \leq 0, \quad \forall t \geq 0,$$
(13)

 $\forall i \in \mathcal{N}^{\text{SE}}$, where

$$\sum_{i \in \mathcal{N}^{\text{SE}}} w_{\mathcal{N}^{\text{SE}}}^i = 1, \quad w_{\mathcal{N}^{\text{SE}}}^i \in \mathbb{R}, \tag{14}$$

and α is a locally Lipschitz class \mathcal{K} function, then $V_{\mathcal{N}^{\text{SE}}}(\{x_i\}_{i\in\mathcal{N}^{\text{SE}}},t)$ asymptotically converges to 0.

Proof. Summing (13) over $i \in \mathcal{N}^{SE}$ yields

$$\sum_{i \in \mathcal{N}^{\text{SE}}} \sup_{\zeta_i \in \partial_{x_i}^{\circ} V_{\mathcal{N}^{\text{SE}}}} \zeta_i \dot{x}_i + \frac{\partial}{\partial t} V_{\mathcal{N}^{\text{SE}}} (\{x_i\}_{i \in \mathcal{N}^{\text{SE}}}, t) + \alpha (V_{\mathcal{N}^{\text{SE}}} (\{x_i\}_{i \in \mathcal{N}^{\text{SE}}}, t)) \le 0, \quad \forall t \ge 0.$$

We also have

$$\begin{split} &L_{X_{\mathcal{N}^{\mathrm{SE}}}}^{\circ}V_{\mathcal{N}^{\mathrm{SE}}}(\{x_{i}\}_{i\in\mathcal{N}^{\mathrm{SE}}},t)\\ &=\sup_{\zeta\in\partial_{x_{\mathcal{N}^{\mathrm{SE}}}}^{\circ}V_{\mathcal{N}^{\mathrm{SE}}}}\zeta\,\dot{x}_{\mathcal{N}^{\mathrm{SE}}}\\ &=\sup_{\zeta\in\partial_{x_{\mathcal{N}^{\mathrm{SE}}}}^{\circ}V_{\mathcal{N}^{\mathrm{SE}}}}\sum_{i\in\mathcal{N}^{\mathrm{SE}}}\zeta_{i}\,\dot{x}_{i}\\ &\leq\sum_{i\in\mathcal{N}^{\mathrm{SE}}}\sup_{\zeta\in\partial_{x_{\mathcal{N}^{\mathrm{SE}}}}^{\circ}V_{\mathcal{N}^{\mathrm{SE}}}}\zeta_{i}\,\dot{x}_{i} =\sum_{i\in\mathcal{N}^{\mathrm{SE}}}\sup_{\zeta_{i}\in\partial_{x_{i}}^{\circ}V_{\mathcal{N}^{\mathrm{SE}}}}\zeta_{i}\,\dot{x}_{i}, \end{split}$$

where $\mathcal{N}^{\mathrm{SE}} = \{i_1, \dots, i_{|\mathcal{N}^{\mathrm{SE}}|}\}$ with $|\mathcal{N}^{\mathrm{SE}}|$ denoting the cardinality of $\mathcal{N}^{\mathrm{SE}}$, $x_{\mathcal{N}^{\mathrm{SE}}} = [x_{i_1}^\top, \dots, x_{i_{|\mathcal{N}^{\mathrm{SE}}|}}^\top]^\top$, and $X_{\mathcal{N}^{\mathrm{SE}}} = [X_{i_1}^\top, \dots, X_{i_{|\mathcal{N}^{\mathrm{SE}}|}}^\top]^\top$. Hence, we can obtain

$$\begin{split} L_{X_{\mathcal{N}^{\text{SE}}}}^{\circ} V_{\mathcal{N}^{\text{SE}}}(\{x_i\}_{i \in \mathcal{N}^{\text{SE}}}, t) + \frac{\partial}{\partial t} V_{\mathcal{N}^{\text{SE}}}(\{x_i\}_{i \in \mathcal{N}^{\text{SE}}}, t) \\ + \alpha(V_{\mathcal{N}^{\text{SE}}}(\{x_i\}_{i \in \mathcal{N}^{\text{SE}}}, t)) \leq 0, \quad \forall t \geq 0. \end{split}$$

By Theorem III.1, this concludes the proof.

The controller $u_i(\{x_i\}_{i\in\mathcal{N}^{\mathrm{SE}}},t)$ for each Agent i can be synthesized in a decentralized manner through an optimization framework as follows, with u_i as a decision variable and (13) as a constraint (which is why the strategy in Theorem IV.1 is called constraint allocation).

$$\underset{u_i \in \mathcal{U}_i}{\operatorname{arg \, min}} \ H_i(u_i, \{x_i\}_{i \in \mathcal{N}^{\text{SE}}}, t)$$

s.t.
$$\max_{\zeta_{i} \in \partial_{x_{i}}^{\circ} V_{\mathcal{N}^{SE}}} \zeta_{i} \dot{x}_{i} + w_{\mathcal{N}^{SE}}^{i} \left(\frac{\partial}{\partial t} V_{\mathcal{N}^{SE}} + \alpha \left(V_{\mathcal{N}^{SE}} \right) \right) \leq 0,$$
(15)

 $\forall i \in \mathcal{N}^{\text{SE}}, \forall t \geq 0$, where $H_i : \mathcal{U}_i \times \mathbb{R}^{\sum_{i \in \mathcal{N}^{\text{SE}}} n_i} \times \mathbb{R}_{\geq 0} \to \mathbb{R}$, and the arguments are omitted for notational simplicity. The priority coefficient $w_{\mathcal{N}^{\text{SE}}}^i$ satisfying (14) assigns the relative

tightness of each constraint according to its importance or priority, or each agent's characteristics or capabilities. Depending on the requirements or preferences of a specific task, such priority coefficients can be fixed, state-dependent, or timevarying, and they can be predefined, adaptively updated, or learned online in practice.

Next, we define the other type of entangled TV-CLFs (which is currently more frequently encountered in multi-robot control) as follows.

Definition IV.2. For each $i \in \mathcal{N}$, let $\mathcal{N}_i^{\mathrm{PE}} \subseteq \mathcal{N} \setminus \{i\}$ denote the neighbor set of Agent i in the Private-Entangled graph $(PE \ graph) \ \mathcal{G}^{\mathrm{PE}} = (\mathcal{N}, \mathcal{E}^{\mathrm{PE}})$, where $\mathcal{E}^{\mathrm{PE}}$ is the set of edges that can be directed or undirected. An NS-TV-CLF

$$V_i^{\mathrm{PE}}: \mathbb{R}^{n_i + \sum_{j \in \mathcal{N}_i^{\mathrm{PE}}} n_j} \times \mathbb{R}_{>0} \to \mathbb{R}_{>0}$$
 (16)

is called a Private-Entangled NS-TV-CLF (PE-NS-TV-CLF) if it depends only on x_i , $\{x_j\}_{j\in\mathcal{N}_i^{\mathrm{PE}}}$, and t.

According to Definition IV.2, if the underlying PE graph $\mathcal{G}^{\mathrm{PE}}$ of a multi-agent task has certain special topologies, then Theorem III.1 can be implemented in a decentralized manner directly. For example, when the PE graph is a finite directed acyclic graph, i.e., each vertex has at most one indegree and one out-degree, with exactly one start vertex and one end vertex, then Theorem III.1 can be implemented in a decentralized manner from one agent to the next sequentially. However, our ambition is to develop a general framework of decentralized control for multi-agent systems that can be applied to deal with any types of underlying graph topologies. To this end, we propose the following theorem that does not rely on any particular topology of the PE graph.

Theorem IV.2. If each agent is executing the time-varying state-feedback controller $u_i(x_i, \{x_i\}_{i \in \mathcal{N}^{PE}}, t)$ such that

$$\sup_{\nu_{i} \in \partial_{x_{i}}^{\circ} V} \nu_{i} \dot{x}_{i} + \frac{\partial}{\partial t} V_{i}^{\text{PE}}(x_{i}, \{x_{j}\}_{j \in \mathcal{N}_{i}^{\text{PE}}}, t)
+ \alpha \left(V_{i}^{\text{PE}}(x_{i}, \{x_{j}\}_{j \in \mathcal{N}_{i}^{\text{PE}}}, t) \right) \leq 0, \quad \forall t \geq 0, \quad (17)$$

 $\forall i \in \mathcal{N}, where$

$$V(x,t) = \sum_{i \in \mathcal{N}} V_i^{\text{PE}}(x_i, \{x_j\}_{j \in \mathcal{N}_i^{\text{PE}}}, t), \tag{18}$$

and α is a locally Lipschitz subadditive class K function, then V(x(t),t) asymptotically converges to 0.

Proof. According to (18), summing (17) over $i \in \mathcal{N}$ yields

$$\sum_{i \in \mathcal{N}} \sup_{\nu_i \in \partial_{x_i}^{\circ} V} \nu_i \, \dot{x}_i + \frac{\partial}{\partial t} V(x, t)$$

$$+ \sum_{i \in \mathcal{N}} \alpha \left(V_i^{\text{PE}}(x_i, \{x_j\}_{j \in \mathcal{N}_i^{\text{PE}}}, t) \right) \leq 0, \quad \forall t \geq 0.$$

Since

$$\begin{split} L_X^{\circ}V(x,t) &= \sup_{\nu \in \partial_x^{\circ}V} \nu \, \dot{x} = \sup_{\nu \in \partial_x^{\circ}V} \sum_{i \in \mathcal{N}} \nu_i \, \dot{x}_i \\ &\leq \sum_{i \in \mathcal{N}} \sup_{\nu \in \partial_x^{\circ}V} \nu_i \, \dot{x}_i = \sum_{i \in \mathcal{N}} \sup_{\nu_i \in \partial_{x_i}^{\circ}V} \nu_i \, \dot{x}_i, \end{split}$$

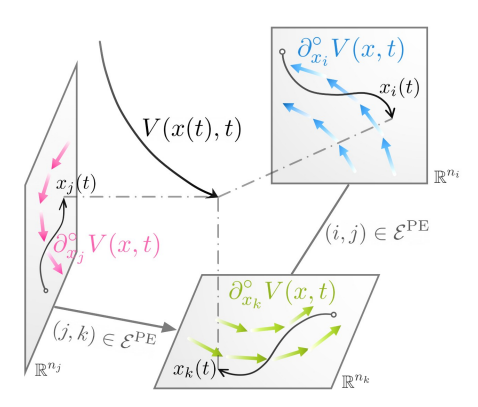


Figure 2. Illustration of the control synthesis framework (19), where the edge (i.j) is undirected while (j,k) is directed.

where $X = [X_1^\top, \dots, X_N^\top]^\top$, then we can obtain

$$L_X^{\circ}V(x,t) + \frac{\partial}{\partial t}V(x,t) + \sum_{i \in \mathcal{N}} \alpha \left(V_i^{\text{PE}}(x_i, \{x_j\}_{j \in \mathcal{N}_i^{\text{PE}}}, t) \right) \leq 0, \quad \forall t \geq 0.$$

Since α is assumed to be a subadditive class K function here, we have

$$L_X^{\circ}V(x,t) + \frac{\partial}{\partial t}V(x,t) + \alpha(V(x,t)) \le 0, \quad \forall t \ge 0.$$

Hence, using Theorem III.1, the proof is completed. \Box

Also, Theorem IV.2 can be utilized for control synthesis through the following optimization framework, as illustrated in Fig. 2.

$$\underset{u_{i} \in \mathcal{U}_{i}}{\operatorname{arg \, min}} \quad H_{i}(u_{i}, x_{i}, \{x_{j}\}_{j \in \mathcal{N}_{i}^{\operatorname{PE}}}, t)$$
s.t.
$$\underset{\nu_{i} \in \partial_{x_{i}}^{\circ} V}{\operatorname{max}} \nu_{i} \, \dot{x}_{i} + \frac{\partial}{\partial t} V_{i}^{\operatorname{PE}} + \alpha \left(V_{i}^{\operatorname{PE}} \right) \leq 0,$$
(19)

 $\forall i \in \mathcal{N}, \forall t \geq 0$, where $H_i : \mathcal{U}_i \times \mathbb{R}^{n_i + \sum_{j \in \mathcal{N}_i^{\text{PE }}} n_j} \times \mathbb{R}_{\geq 0} \to \mathbb{R}$, and the arguments are omitted for notational simplicity.

Remark IV.1. Although the constraint in the optimization problem (19) is another optimization problem, it is linear in ν_i constraint to a Clarke generalized gradient (and thus sup coincides with max), so it suffices to enforce finite number of boundary elements (which are standard gradients) in such convex hull (see, e.g., [32], [34]), instead of considering an infinite dimensional nested optimization problem. This also applies to the optimization problem (15).

In a multi-agent task, an agent may be involved in a PE graph and some SE graphs simultaneously. As such, we propose the *disentangled control* as follows. By *disentangled* we mean a decentralized control synthesis framework in the presence of entangled dynamics in multi-agent systems.

$$\underset{u_{i} \in \mathcal{U}_{i}}{\operatorname{arg \, min}} \ H_{i}(u_{i}, x_{i}, \{x_{j}\}_{j \in \mathcal{N}_{i}^{\mathrm{PE}}}, \{x_{j}\}_{j \in \mathcal{N}_{i}^{\mathrm{SE}}}, t)$$

$$\text{s.t.} \ \underset{\nu_{i} \in \partial_{x_{i}}^{\circ} V}{\max} \nu_{i} \dot{x}_{i} + \frac{\partial}{\partial t} V_{i}^{\mathrm{PE}} + \alpha \left(V_{i}^{\mathrm{PE}}\right) \leq 0$$

$$\underset{\zeta_{i} \in \partial_{x_{i}}^{\circ} V_{\mathcal{N}^{\mathrm{SE}}}}{\max} \zeta_{i} \dot{x}_{i} + w_{\mathcal{N}^{\mathrm{SE}}}^{i} \left(\frac{\partial}{\partial t} V_{\mathcal{N}^{\mathrm{SE}}} + \alpha \left(V_{\mathcal{N}^{\mathrm{SE}}}\right)\right) \leq 0$$

 $\forall \mathcal{N}^{\text{SE}} \in \mathcal{S}^{\text{SE}}, \ \forall i \in \mathcal{N}, \ \forall t \geq 0, \ \text{where} \ H_i : \mathcal{U}_i \times \mathbb{R}^{n_i} \times \mathbb{R}^{\sum_{j \in \mathcal{N}_i^{\text{PE}}} n_j} \times \mathbb{R}^{\sum_{j \in \mathcal{N}_i^{\text{SE}}} n_j} \times \mathbb{R}_{\geq 0} \to \mathbb{R}, \ \text{and the arguments}$ are omitted for notational simplicity.

Remark IV.2. The advantages of the disentangled control (20) are as follows.

- It is decentralized in the sense that when Agent i, for any $i \in \mathcal{N}$, computes its control input u_i , it does not need any simultaneous neighbor control input u_j whose computation, in turn, relies on u_i .
- It is applicable to PE graphs of any types of topologies, i.e., directed graph, undirected graph, mixed graph, and piecewise-constant graph. (The SE graph is complete by definition.)
- If H_i is quadratic in u_i, since the constraints in (20) are linear in u_i, then (20) becomes a quadratic program (which offers fast computation) and thus is ideal for realtime applications, such as robotics in complex environments, where rapid adaptation and decision-making are crucial.
- It naturally accommodates simultaneous consideration of multiple objectives, as any additional constraint that encodes a certain objective can be plugged into (20), where slack variables may be incorporated in case of conflict among different constraints.

The disentangled control (20) provides a general solution to a wide variety of multi-agent tasks, as it not only solves the problems that can be addressed by existing methods, but also solves problems beyond their reach, such as the long-standing open problem, decentralized coverage control for time-varying density functions without resorting to any simplifying approximations, which will be demonstrated in detail in the following section.

V. APPLICATIONS AND EXPERIMENTS

In this section, we apply the results developed in Section IV with $H_i = \|u_i\|^2$, $f_i = 0$, $g_i = I$, $\forall i \in \mathcal{N}$, to a team of mobile robots, a common object in multi-agent studies, for different tasks, where the state of interest refers to the positions of the robots (with $n_i = 2$ for planar robots and $n_i = 3$ for aerial robots). For physical experiments, we utilize a group of differential-drive mobile robots in a rectangular domain $\mathcal{D} \subset \mathbb{R}^2$ with x-axis ranging from -1.6 to 1.6 meters and y-axis ranging from -1 to 1 meter [42]. Each robot operates with the help of the near-identity diffeomorphism [43]. Note that all the applications demonstrated in this section cannot be theoretically addressed with rigorous convergence guarantees under the methods proposed in [15], [22], which will be explained in detail in Appendix A.

A. Time-Varying Leader-Follower Formation Control

In this subsection, we implement the proposed disentangled control in simulation for time-varying leader-follower formation control, which can be applied in collaborative transportation in space, object caging or containment, swarm robotic art performance, etc.

Specifically, we consider N=13 robots with twelve followers, whose states are denoted by $x_i \in \mathbb{R}^3$, $\forall i \in \mathcal{N} \setminus \{\ell\}$, and one leader, whose state is denoted by $x_\ell \in \mathbb{R}^3$ with $\ell=13$. The goal is that the follower robots form a regular icosahedron of time-varying size, containing the leader robot in its geometric center. To this end, the PE-TV-CLF for each follower robot is defined as

$$V_{i}^{\text{PE}}(x_{i}, \{x_{j}\}_{j \in \mathcal{N}_{i}^{\text{PE}}}, t) = \frac{w^{\text{f}}}{2} \sum_{j \in \mathcal{N}_{i}^{\text{PE}} \setminus \{\ell\}} (\|x_{i} - x_{j}\| - d_{ij}(t))^{2} + \frac{w^{\ell}}{2} (\|x_{i} - x_{\ell}\| - d_{i}^{\ell}(t))^{2}, \quad (21)$$

 $\forall i \in \mathcal{N} \setminus \{\ell\}$, where the PE graph consists of the vertices representing the follower robots and edges of a regular icosahedron, augmented with an additional vertex representing the leader and directed edges from the leader to each follower, $d_{ij}(t)>0$ denotes the edge length at time $t,d_i^\ell(t)>0$ denotes the circumradius (i.e., the distance from the geometric center to a vertex) at time t, and the weighting coefficients $w^f>0$ and $w^\ell>0$ determine the relative importance of achieving the goals between maintaining the time-varying formation and following the leader.

According to (21), we can obtain

$$\nabla_{x_{i}}V = 2w^{f} \sum_{j \in \mathcal{N}_{i}^{PE} \setminus \{\ell\}} \frac{\|x_{i} - x_{j}\| - d_{ij}}{\|x_{i} - x_{j}\|} (x_{i} - x_{j})^{\top} + w^{\ell} \frac{\|x_{i} - x_{\ell}\| - d_{i}^{\ell}}{\|x_{i} - x_{\ell}\|} (x_{i} - x_{\ell})^{\top}$$

$$(22)$$

and

$$\frac{\partial}{\partial t} V_i^{\text{PE}} = w^{\text{f}} \sum_{j \in \mathcal{N}_i^{\text{PE}} \setminus \{\ell\}} (d_{ij} - \|x_i - x_j\|) \dot{d}_{ij}
+ w^{\ell} (d_i^{\ell} - \|x_i - x_{\ell}\|) \left(\frac{(x_i - x_{\ell})^{\top}}{\|x_i - x_{\ell}\|} \dot{x}_{\ell} + \dot{d}_i^{\ell} \right)$$
(23)

 $\forall i \in \mathcal{N} \setminus \{\ell\}$, where the arguments are omitted for notational simplicity. Note that the time-varying leader-follower formation control by using the proposed framework is decentralized because when Robot i, for any $i \in \mathcal{N} \setminus \{\ell\}$, computes its control input u_i , it only needs the states of itself and its neighbors, and the velocity of the leader robot available through sensing, as seen in (21), (22), and (23).

Since the topology of the underlying PE graph is constant, the Clarke generalized gradient degenerates to the standard gradient. Substituting (21), (22), and (23) into (19) (as there is no SE graph involved in this application), the simulation results are shown in Fig. 3, Fig. 4, and Fig. 5. The results show that the total PE-TV-CLF of the follower robots $V^{\mathrm{PE}}(x,t) = \sum_{i \in \mathcal{N}\setminus \{\ell\}} V_i^{\mathrm{PE}}(x_i, \{x_j\}_{j \in \mathcal{N}_i^{\mathrm{PE}}, t}) \text{ converges to 0 at around time step 300 and maintain at 0 thereafter, i.e.,}$

the twelve follower robots converge to the formation of regular icosahedron of time-varying size and contain the leader robot in the center of the icosahedron, which verifies Theorem IV.2. (We omit discussion of the individual TV-CLF for the leader robot, as it does not depend on the state of any follower robots and is assumed to always converge to zero.)

Notably, we observe from Fig. 5 (together with Fig. 4) that an interesting phenomenon emerges spontaneously (i.e., without the imposition of certain predefined rules aimed at producing it): To ensure the decrease of the total PE-TV-CLF $V^{\rm PE} = \sum_{i \in \mathcal{N} \setminus \{\ell\}} V_i^{\rm PE}$, some follower robots occasionally "sacrifice" by allowing their individual PE-TV-CLFs $V_i^{\rm PE}$ to increase druing some period of time (e.g., Robot 9 from around time steps 15 to 35 and 100 to 150), thereby contributing to the "greater good" of the whole system.

B. Decentralized Coverage Control for Time-Varying Density Functions

In this subsection, we apply the disentangled control to solve the long-standing challenge: decentralized coverage control for time-varying density functions (without any approximations), which can be applied in environmental monitoring, target tracking, search-and-rescue, etc.

To start with, the (time-invariant) coverage control [11] concerns the problem of minimizing

$$C(x) = \sum_{i \in \mathcal{N}} \int_{\mathcal{V}_i(x)} ||x_i - q||^2 \rho(q) \, \mathrm{d}q$$
 (24)

encoding the lack of coverage quality of a domain of interest $\mathcal{D} \subset \mathbb{R}^{n_i}$, where

$$\mathcal{V}_i(x) = \left\{ q \in \mathcal{D} \mid ||q - x_i|| \le ||q - x_j||, \ \forall j \in \mathcal{N} \setminus \{i\} \right\}$$

is the Voronoi cell of Agent i, and $\rho: \mathbb{R}^{n_i} \to \mathbb{R}_{\geq 0}$ is a density distribution function encoding the relative importance or informativeness of a point $q \in \mathcal{D}$. According to [11], $\nabla_{x_i} C(x) = 2M_i(x)(x_i - G_i(x))^{\top}$, where

$$M_i(x) = \int_{\mathcal{V}_i(x)} \rho(q) \, \mathrm{d}q, \quad G_i(x) = \frac{\int_{\mathcal{V}_i(x)} q\rho(q) \, \mathrm{d}q}{M_i(x)}$$
 (25)

are the mass and center of mass of $\mathcal{V}_i(x)$, respectively. Note that the set $\{q \in \mathcal{D} \mid \rho(q) = 0\}$ must be nonidentical to $\mathcal{V}_i(x)$, $\forall i \in \mathcal{N}$, to ensure that $G_i(x)$ is well-defined. The gradient flow method [11] (also known as the continuous-time limit of Lloyd's algorithm [44]), ensures asymptotic convergence to a critical point of C(x) with respect to x (guaranteed by LaSalle's invariance principle), i.e., a centroidal Voronoi tessellation (CVT),

$$x_i^* = G_i(x^*), \quad \forall i \in \mathcal{N}.$$
 (26)

When the density distribution function becomes time-varying, i.e., $\rho: \mathbb{R}^{n_i} \times \mathbb{R}_{\geq 0} \to \mathbb{R}_{\geq 0}$, the gradient flow method (or Lloyd's algorithm) does not guatanee the convergence to a time-varying CVT (TV-CVT), as analyzed in [19]. In this time-varying setting, the corresponding locational cost function takes the form of

$$C(x,t) = \sum_{i \in \mathcal{N}} \int_{\mathcal{V}_i(x)} ||x_i - q||^2 \rho(q,t) \,\mathrm{d}q.$$

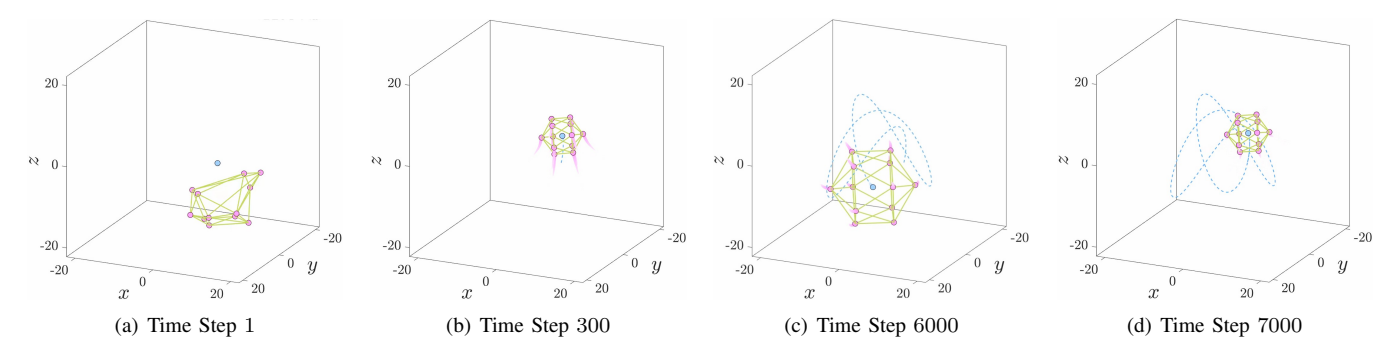


Figure 3. Snapshots of the simulation of decentralized time-varying leader-follower formation control in Section V-A. The twelve follower robots are represented by the pink dots, while the leader robot is represented by the blue dot. The green lines represent the undirected edges of the corresponding PE graph, and the blue dashed line represents the trajectory traveled by the leader robot. The full video of this simulation is available online at https://youtu.be/DyY8JiIXzAc.

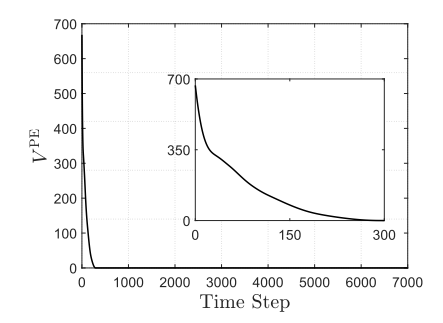


Figure 4. The evolution of the total PE-TV-CLF of the follower robots defined in Section V-A with respect to time steps.

However, it is challenging to ensure convergence to a TV-CVT in a decentralized manner. Existing state-of-theart methods typically rely on certain simplifying approximations to achieve decentralized implementations. For example, [45] requires the quasi-static approximations of $\frac{d}{dt}G_i(x,t),$ $\frac{d}{dt}M_i(x,t),$ and $\frac{\partial}{\partial t}\rho(q,t),$ and [19] relies on truncated Neumann series approximations. Despite the progress in the community, decentralized coverage control for time-varying densities with rigorous convergence guarantees without resorting to approximations remains a challenging open problem that, to the best of our knowledge, has not yet been resolved, even setting aside the treatment of the nonsmooth issue caused by the associated piecewise-constant Delaunay graph.

Nevertheless, our proposed framework can solve this problem by formulating the PE-NS-TV-CLF for each robot as

$$V_i^{\text{PE}}(x_i, \{x_j\}_{j \in \mathcal{N}_i^{\text{PE}}}, t) = \frac{1}{2} \|x_i - G_i(x_i, \{x_j\}_{j \in \mathcal{N}_i^{\text{PE}}}, t)\|^2,$$
(27)

 $\forall i \in \mathcal{N}$, where the PE-graph is the Delaunay graph. Precisely,

$$G_i(x_i, \{x_j\}_{j \in \mathcal{N}_i^{\text{PE}}}, t) = \frac{\int_{\mathcal{V}_i(x_i, \{x_j\}_{j \in \mathcal{N}_i^{\text{PE}}})} q \rho(q, t) \, \mathrm{d}q}{M_i(x_i, \{x_j\}_{j \in \mathcal{N}_i^{\text{PE}}}, t)},$$

in which

$$M_i(x_i, \{x_j\}_{j \in \mathcal{N}_i^{\text{PE}}}, t) = \int_{\mathcal{V}_i(x_i, \{x_j\}_{j \in \mathcal{N}_i^{\text{PE}}})} \rho(q, t) \, \mathrm{d}q.$$

According to (27), we can obtain

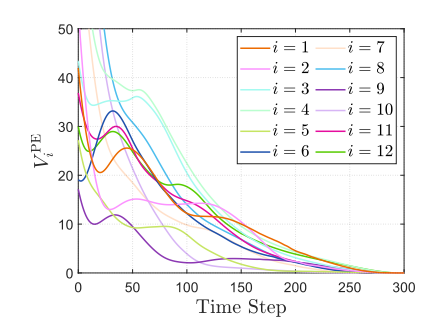


Figure 5. The evolution of the PE-TV-CLF for each follower robot defined in Section V-A with respect to time steps.

$$\frac{\partial}{\partial t} V_i^{\text{PE}} = \frac{1}{M_i} (G_i - x_i)^{\top} \int_{\mathcal{V}_i} (q - G_i) \frac{\partial}{\partial t} \rho \, \mathrm{d}q, \qquad (28)$$

and

$$\nabla_{x_i} V = (x_i - G_i)^{\top} \left(I - \frac{\partial G_i}{\partial x_i} \right) + \sum_{j \in \mathcal{N}_i^{\text{PE}}} (G_j - x_j)^{\top} \frac{\partial G_j}{\partial x_i},$$
(29)

in which the Jacobians are

$$\frac{\partial G_i}{\partial x_i} = \sum_{j \in \mathcal{N}_i^{\text{PE}}} \frac{\int_{\partial \mathcal{V}_{ij}} (q - G_i) (q - x_i)^{\top} \rho \, \mathrm{d}q}{M_i \|x_j - x_i\|},$$

$$\frac{\partial G_j}{\partial x_i} = \frac{\int_{\partial \mathcal{V}_{ij}} (G_j - q)(q - x_i)^\top \rho \, \mathrm{d}q}{M_i \|x_i - x_i\|},$$

with $\partial \mathcal{V}_{ij} = \{q \in \mathcal{D} \mid ||q - x_i|| = ||q - x_j||\}$, where the arguments in (28) and (29) are omitted for notational simplicity.

It can be seen from (27), (28), and (29) that the coverage control for time-varying density functions by using the proposed framework is decentralized. This is because when Agent i, for any $i \in \mathcal{N}$, computes its control input u_i , it only needs the states of itself and its neighbors, and the density distribution ρ and the density dynamics $\frac{\partial}{\partial t}\rho$ in its dominant subdomain \mathcal{V}_i . Moreover, no simplifying approximation, such as Neumann series truncations, is involved, and the convergence to a TV-CVT,

$$x_i^*(t) = G_i(x^*(t), \{x_j^*(t)\}_{j \in \mathcal{N}_i^{\text{PE}}}, t), \quad \forall i \in \mathcal{N},$$
 (30)

is rigorously guaranteed by Theorem IV.2. Note that as highlighted in Remark IV.1, it suffices to enforce the boundary

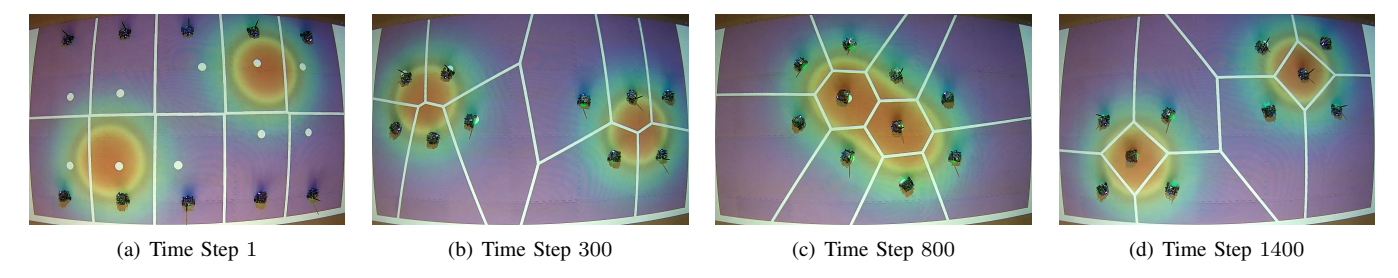


Figure 6. Snapshots of the physical experiment of decentralized coverage control for time-varying density distribution in Section V-B. Each robot is in charge of a dominant subdomain, i.e., a Voronoi cell, with a set of white lines as its boundaries and a white dot as its center of mass with respect to the time-varying density distribution. A rainbow colormap is employed to visualize this density distribution, with warmer colors representing higher density values and cooler colors representing lower values. The full video of this experiment is available online at https://youtu.be/eyFkZO9CuQ0.

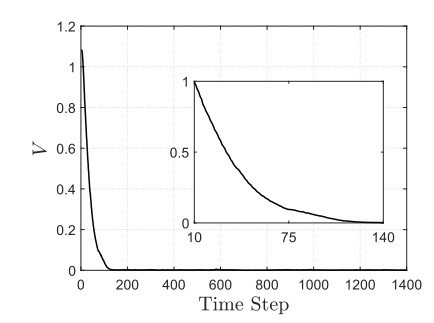


Figure 7. The evolution of the total PE-NS-TV-CLF defined in Section V-B with respect to time steps.

elements in the Clarke generalized gradient, i.e., the standard gradients (29) with different sets of bisectors ∂V_{ij} due to the underlying piecewise-constant Delaunay graph.

In the physical experiment, we use a group of N=10 differential-drive mobile robots. The initial configuration of the robots is shown in Fig. 6(a), where \mathcal{V}_i and G_i , for any $i \in \mathcal{N}$, is represented by a white dots and a set of white lines respectively, and the density $\rho(q,t)$ is visualized by a rainbow colormap with warmer colors corresponding to higher density values and cooler colors to lower values.

Substituting (27), (28), and (29) into (19) (since there is no SE graph involved in this application), the experimental results are shown in Fig. 6 and Fig. 7. As shown in Fig. 7, the total PE-NS-TV-CLF $V(x,t) = \sum_{i \in \mathcal{N}} V_i^{\text{PE}}(x_i, \{x_j\}_{j \in \mathcal{N}_i^{\text{PE}}}, t)$ converges to 0 at around time step 140 and maintains at 0 thereafter, i.e., the team of robots converge to and maintain a TV-CVT (30), as can also be seen in Fig. 6, which verifies Theorem IV.2.

C. Safe Formation Navigation in a Dense Environment

As hilighted in Remark IV.2, an advantage of the proposed disentangled control (20) is that it naturally accommodates multi-objective robotic tasks through incorporating the corresponding constraints. To demonstrate this benefit, in this subsection, we consider the objective of collision avoidance in addition to navigation in formation.

Specifically, we consider N=5 agents with four follower robots, whose states are denoted by $x_i \in \mathbb{R}^2$, $\forall i \in \mathcal{N} \setminus \{\ell\}$, and one virtual leader, whose state is denoted by $x_\ell \in \mathbb{R}^2$

with $\ell=5$. The goal is that the follower robots form a square and follow the virtual leader in its geometric center as much as possible, while avoiding collisions in an environment with dense circular obstacles. To this end, the PE-CLF for each follower robot is defined as

$$V_i^{\text{PE}}(x_i, \{x_j\}_{j \in \mathcal{N}_i^{\text{PE}}}) = \frac{w^{\text{f}}}{2} \sum_{j \in \mathcal{N}_i^{\text{PE}} \setminus \{\ell\}} (\|x_i - x_j\| - d_{ij})^2 + \frac{w^{\ell}}{2} (\|x_i - x_\ell\| - d_i^{\ell})^2, \quad (31)$$

which is the time-invariant version of (21), $\forall i \in \mathcal{N} \setminus \{\ell\}$, where the PE graph consists of the vertices representing the follower robots and edges of a square, augmented with an additional vertex representing the virtual leader and directed edges from the leader to each follower.

Since each robot has to avoid colliding with obstacles and safety is typically more important than task accomplishment, a slack variable should be added into the constraint induced by (31). Thus, unlike the constraint induced by (27) that naturally prevents each robot from colliding with other robots in the task in Section V-B (thanks to the Voronoi tessellation), due to the slack variable introduced into the constraint induced by (31), collision avoidance between robots should also be taken into account. Hence, we set two additional types of constraints for each robot to ensure that it neither collides with obstacles nor with any other robots.

The CBF for Robot i to avoid colliding with Obstacle $k \in \mathcal{K} \coloneqq [1,2,\ldots,K]$ with $K \in \mathbb{Z}^+$ is given by $h_i^k(x_i) = \|x_i - c_k\|^2 - r_k^2$, where $c_k \in \mathbb{R}^2$ and $r_k > 0$ are the center and radius of Obstacle k respectively. The corresponding CBF-induced constraint can be directly obtained using Lemma III.2. In addition, the CBF for Robot i to avoid colliding with Robot i is defined as

$$h_{ij}^{SE}(x_i, x_j) = ||x_i - x_j||^2 - D_{ij}^2,$$
 (32)

where $D_{ij} > 0$ is the safe distance between Robots i and j. Note that (32) is a shared-entangled CBF (SE-CBF) that involves the states of both Robots i and j, as defined below.

Definition V.1. Given an SE graph $\mathcal{G}^{SE} = (\mathcal{N}^{SE}, \mathcal{E}^{SE})$ per Definition IV.1, a CBF $h_{\mathcal{N}^{SE}} : \mathbb{R}^{\sum_{i \in \mathcal{N}^{SE}} n_i} \to \mathbb{R}$ is called an SE-CBF if it depends only on $\{x_i\}_{i \in \mathcal{N}^{SE}}$.

Thus, the constraint allocation strategy in (15), adapted into the formulation of CBF, can be utilized to achieve decentral-









(a) Time Step 1

(b) Time Step 500

(c) Time Step 1000

(d) Time Step 2000

Figure 8. Snapshots of the physical experiment for safe formation navigation in a dense environment in Section V-C. The magenta lines represent the undirected edges of the corresponding PE graph, the blue disks represent the obstacles, and the green dashed curves represent the trajectories of the robots traveled up to time step 2000. The full video of this experiment is available online at https://youtu.be/CMFtsuBCy0k.

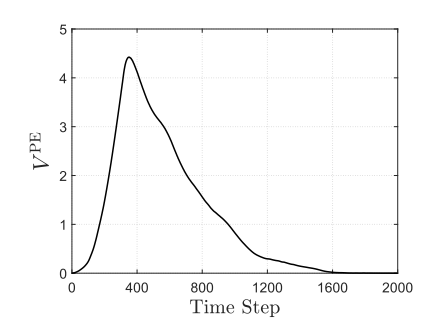


Figure 9. The evolution of the total PE-CLF of the follower robots defined in Section V-C with respect to time steps.

ized implementation. Specifically, the framework (20) with the time-invariant setting and slack variables in this subsection takes the form of

$$\begin{aligned} \underset{u_{i} \in \mathcal{U}_{i}, \, \delta_{i} \in \mathbb{R}}{\operatorname{arg\,min}} \|u_{i}\|^{2} + \kappa_{i} \delta_{i}^{2} \\ \text{s.t.} \quad & \nabla_{x_{i}} V \, u_{i} \leq -\alpha \left(V_{i}^{\operatorname{PE}}\right) + \delta_{i} \\ & (x_{i} - x_{j})^{\top} u_{i} \geq -w_{\mathcal{N}^{\operatorname{SE}}}^{i} \, \gamma(h_{ij}^{\operatorname{SE}}), \ \, \forall j \in \mathcal{N} \backslash \{i, \ell\}, \\ & (x_{i} - c_{k})^{\top} u_{i} \geq -\gamma(h_{i}^{k}), \ \, \forall k \in \mathcal{K}, \end{aligned}$$

 $\forall i \in \mathcal{N} \setminus \{\ell\}$, where $\kappa_i > 0$ is a penalty coefficient, and an additional CLF-induced constraint with a slack variable is added when i = 2 to regulate the orientation of the formation.

The initial configuration of four differential-drive mobile robots is shown in Fig. 8(a). The experimental results are shown in Fig. 8 and Fig. 9, from which one can observe that at the beginning and from around time step 1600 to 2000, the four robots are in the desired square formation, i.e., the corresponding total PE-CLF of the follower robots $V^{\rm PE}(x) = \sum_{i \in \mathcal{N}\setminus \{\ell\}} V_i^{\rm PE}(x_i, \{x_j\}_{j \in \mathcal{N}_i^{\rm PE}})$ is zero. However, when the robots are navigating through the densely distributed obstacles, due to the priority of safety (i.e., collision avoidance), they cannot maintain a perfect formation, which is why the total PE-CLF $V^{\rm PE}$ is nonzero during this period of time. In addition, the trajectories of the robots, represented by the green dashed curves shown in Fig. 8(d), indicate that the safety is ensured throughout the experiment.

VI. CONCLUSIONS

In this paper, we developed a general multi-agent control framework, named *disentangled control*. This framework

is broadly applicable, no matter when the underlying PE graph is undirected, directed, or piecewise constant, and provides a systematic way of solving a particularly challenging problem, i.e., decentralization of entangled dynamics among involved agents. For example, it resolves a long-standing open problem that existing methods do not provide rigorous convergence guarantees, i.e., decentralized coverage control for time-varying densities, without relying on any simplifying approximations. Furthermore, the framework is suitable for multi-objective robotics and real-time implementations, as demonstrated in the physical experiments.

Notably, since any objective function that can be constructed in the form of a TV-CLF can be seamlessly integrated into the proposed framework, it can be utilized to solve a wide range of problems in a decentralized manner. To name a few, aerial-ground robotic collaboration where the heterogeneous agents have states of different dimensions, i.e., $n_i \neq n_j$, and decentralized coverage control for multiple different timevarying densities, i.e., $\rho_i(q,t) \neq \rho_j(q,t)$. Extending even beyond robotics, the framework holds significant promise for decentralized decision-making and action generation in multiagent systems. We leave to the community further exploration of the ideas of Theorem IV.1 and Theorem IV.2 in broader fields and more diverse applications.

APPENDIX A LIMITATIONS OF RELATED WORKS

In the appendix, we discuss some missing pieces in [15] and analyze several theoretical limitations of [22] in detail. For terminological consistency, we equivalently rewrite the main results of [15] and [22] in the context of CLF per Remark III.1.

First, we revisit the constraint-driven multi-agent control framework proposed in [15].

Proposition A.1. (A refinement of Proposition 8 in [15]) *Consider the cost function*

$$J(x) = \sum_{i \in \mathcal{N}} \sum_{j \in \mathcal{N}_i} J_{ij}(\|x_i - x_j\|), \tag{33}$$

where \mathcal{N}_i denotes the set of indices of the neighbors of Agent i. If $J_{ij}: \mathbb{R}_{\geq 0} \to \mathbb{R}_{\geq 0}$, $J_{ij}(\|x_i - x_j\|) = J_{ji}(\|x_j - x_i\|)$ is a symmetric, pairwise function between Agents i and j, and each agent is executing the state-feedback controller $u_i(x_i)$ such that

$$\nabla_{x_i} J_i(x(t)) \, \dot{x}_i(t) \le -\alpha(J_i(x(t))), \quad \forall t \ge 0, \tag{34}$$

 $\forall i \in \mathcal{N}$, where $J_i(x) = \sum_{j \in \mathcal{N}_i} J_{ij}(\|x_i - x_j\|)$ and α is a locally Lipschitz subadditive class \mathcal{K} function, then J(x) given by (33) asymptotically converges to 0.

Remark A.1. Proposition A.1 refines Proposition 8 in [15] by eliminating the need for the single-integrator dynamics, the slack variables, and the quadratic program formulation, where Remark III.1 is invoked to recast the CBF formulation as an equivalent CLF formulation (so the superadditivity of α is replaced by the subadditivity).

However, the structural assumptions on the cost function (33) in Proposition A.1 somewhat restrict the classes of systems that can be covered. For example, Proposition A.1 requires the underlying graph to be undirected, but the leader-follower control, even in the time-invariant case, is associated with a directed graph since there is typically no transmission of information from followers to leaders. In addition, Proposition A.1 requires the cost function to be an explicit function of the distance between two agents, but the cost function for coverage control (27), even in the time-invariant case, does not have such property. Nevertheless, Proposition A.1 provides convergence guarantees for consensus control (or rendezvous) and formation control in the time-invariant settings.

Next, we clarify several issues in [22], even setting aside the treatment of piecewise-constant graph topology.

One issue is that when [22] calculates the total time derivatives of some quantities, the influence from the neighbors are missing. For example, [22] formulates the individual cost function of each agent as

$$J_i(x,t) = \frac{1}{2} ||x_i - G_i(x,t)||^2, \quad \forall i \in \mathcal{N},$$
 (35)

where $G_i(x,t)$ is the center of mass of the Voronoi cell of Agent i, and then substitutes it into the framework proposed in [15]. However, Proposition 6 in [22] calculates the total time derivative of (35) as

$$\dot{J}_i(x,t) = \nabla_{x_i} J_i(x,t) \, \dot{x}_i + \frac{\partial}{\partial t} J_i(x,t),$$

which is inaccurate in the context of coverage control because

$$\dot{J}_i(x,t) = \nabla_{x_i} J_i(x,t) \, \dot{x}_i + \sum_{j \in \mathcal{N}_i} \nabla_{x_j} J_i(x,t) \, \dot{x}_j + \frac{\partial}{\partial t} J_i(x,t),$$

where \mathcal{N}_i denotes the Delaunay neighbors of Agent *i*. Note that $\dot{M}_i(x,t) \neq \frac{\partial}{\partial t} M_i(x,t) = \int_{\mathcal{V}_i(x)} \frac{\partial}{\partial t} \rho(x,t) \, \mathrm{d}q$, and likewise

$$\dot{G}_i(x,t) \neq \frac{\partial}{\partial t} G_i(x,t) = \frac{\int_{\mathcal{V}_i(x)} (q - G_i(x,t)) \frac{\partial}{\partial t} \rho(q,t) \, \mathrm{d}q}{M_i(x,t)},$$

because

$$\dot{G}_{i}(x,t) = \frac{\partial G_{i}}{\partial x_{i}}(x,t) \, \dot{x}_{i} + \sum_{j \in \mathcal{N}_{i}} \frac{\partial G_{i}}{\partial x_{j}}(x,t) \, \dot{x}_{j} + \frac{\partial}{\partial t} G_{i}(x,t).$$

Another issue is that the conclusion of Proposition 4 in [22] does not necessarily hold, not only for coverage control, but also for other multi-agent tasks with even relatively simpler forms of $J_i(x,t)$. This is because the convergence condition given by [22] can be equivalently rewritten as

$$\nabla_{x_i} J_i(x,t) \,\dot{x}_i + \frac{\partial}{\partial t} J_i(x,t) \le -\alpha(J_i(x,t)), \qquad (36)$$

where α is a locally Lipschitz subadditive class \mathcal{K} function. One can observe that (36) is the time-varying variance of (34). By summing (36) over all $i \in \mathcal{N}$, we have $\sum_{i \in \mathcal{N}} \nabla_{x_i} J_i(x,t) \dot{x}_i \leq -\frac{\partial}{\partial t} J(x,t) - \alpha(J(x,t))$, which does not imply

$$\dot{J}(x,t) \le -\alpha(J(x,t)), \quad \forall t \ge 0. \tag{37}$$

However, (37) is essential to ensure asymptotic convergence of J(x,t) to 0 per Lemma III.1.

A further issue is that, even in the special case where $J_i(x,t)$ could be written as an explicit function of the distance between two agents, i.e.,

$$J_i(x,t) = \sum_{i \in \mathcal{N}_i} J_{ij}(\|x_i - x_j\|, t), \quad \forall i \in \mathcal{N},$$
 (38)

although the form (38) is in fact not admissible for coverage control, the condition (37) is still not guaranteed by Proposition 4 in [22].

Remark A.2. A special case in which the method proposed in [22] is theoretically guaranteed to converge occurs when

$$\nabla_{x_i} J(x,t) = \nabla_{x_i} J_i(x,t), \quad \forall i \in \mathcal{N}.$$
 (39)

However, the condition (39) is rather restrictive, as it does not hold even in basic multi-agent tasks such as rendezvous.

REFERENCES

- [1] F. Bullo, J. Cortés, and S. Martinez, Distributed control of robotic networks: a mathematical approach to motion coordination algorithms. Princeton University Press, 2009.
- [2] M. Schwager, "A gradient optimization approach to adaptive multirobot control," Ph.D. dissertation, Massachusetts Institute of Technology, Cambridge, MA, 2009.
- [3] R. Olfati-Saber, J. A. Fax, and R. M. Murray, "Consensus and cooperation in networked multi-agent systems," *Proceedings of the IEEE*, vol. 95, no. 1, pp. 215–233, 2007.
- [4] M. Mesbahi and M. Egerstedt, Graph theoretic methods in multiagent networks. Princeton University Press, 2010.
- [5] A. Bidram, A. Davoudi, F. L. Lewis, and Z. Qu, "Secondary control of microgrids based on distributed cooperative control of multi-agent systems," *IET Generation, Transmission & Distribution*, vol. 7, no. 8, pp. 822–831, 2013.
- [6] K. Dresner and P. Stone, "A multiagent approach to autonomous intersection management," *Journal of artificial intelligence research*, vol. 31, pp. 591–656, 2008.
- [7] T. Rashid, M. Samvelyan, C. S. De Witt, G. Farquhar, J. Foerster, and S. Whiteson, "Monotonic value function factorisation for deep multiagent reinforcement learning," *Journal of Machine Learning Research*, vol. 21, no. 178, pp. 1–51, 2020.
- [8] M. Tan, "Multi-agent reinforcement learning: Independent vs. cooperative agents," in *Proceedings of the tenth international conference on machine learning*, 1993, pp. 330–337.
- [9] A. Ghosh, V. Kulharia, V. P. Namboodiri, P. H. Torr, and P. K. Dokania, "Multi-agent diverse generative adversarial networks," in *Proceedings of the IEEE conference on computer vision and pattern recognition*, 2018, pp. 8513–8521.
- [10] M. Egerstedt and X. Hu, "Formation constrained multi-agent control," IEEE Transactions on Robotics and Automation, vol. 17, no. 6, pp. 947– 951, 2001.
- [11] J. Cortes, S. Martinez, T. Karatas, and F. Bullo, "Coverage control for mobile sensing networks," *IEEE Transactions on Robotics and Automation*, vol. 20, no. 2, pp. 243–255, 2004.
- [12] G. A. Pereira, M. F. Campos, and V. Kumar, "Decentralized algorithms for multi-robot manipulation via caging," *The International Journal of Robotics Research*, vol. 23, no. 7-8, pp. 783–795, 2004.
- [13] M. Ji, G. Ferrari-Trecate, M. Egerstedt, and A. Buffa, "Containment control in mobile networks," *IEEE Transactions on Automatic Control*, vol. 53, no. 8, pp. 1972–1975, 2008.

- [14] J. Cortés and M. Egerstedt, "Coordinated control of multi-robot systems: A survey," SICE Journal of Control, Measurement, and System Integration, vol. 10, no. 6, pp. 495–503, 2017.
- [15] G. Notomista and M. Egerstedt, "Constraint-driven coordinated control of multi-robot systems," in 2019 American Control Conference (ACC). IEEE, 2019, pp. 1990–1996.
- [16] M. Farina and R. Scattolini, "Distributed predictive control: A non-cooperative algorithm with neighbor-to-neighbor communication for linear systems," *Automatica*, vol. 48, no. 6, pp. 1088–1096, 2012.
- [17] P. A. Trodden and J. M. Maestre, "Distributed predictive control with minimization of mutual disturbances," *Automatica*, vol. 77, pp. 31–43, 2017
- [18] R. Lin, S. Kim, and M. Egerstedt, "Heterogeneous collaborative pursuit via coverage control driven by Fokker-Planck equations," *IEEE Transactions on Robotics*, vol. 41, pp. 3649 – 3668, 2025.
- [19] S. G. Lee, Y. Diaz-Mercado, and M. Egerstedt, "Multirobot control using time-varying density functions," *IEEE Transactions on Robotics*, vol. 31, no. 2, pp. 489–493, 2015.
- [20] B. T. Stewart, A. N. Venkat, J. B. Rawlings, S. J. Wright, and G. Pannocchia, "Cooperative distributed model predictive control," *Systems & Control Letters*, vol. 59, no. 8, pp. 460–469, 2010.
- [21] B. A. Butler, C. H. Leung, and P. E. Paré, "Collaborative safety-critical formation control with obstacle avoidance," arXiv preprint arXiv:2410.03885, 2024.
- [22] M. Santos, S. Mayya, G. Notomista, and M. Egerstedt, "Decentralized minimum-energy coverage control for time-varying density functions," in 2019 International Symposium on Multi-Robot and Multi-Agent Systems (MRS). IEEE, 2019, pp. 155–161.
- [23] P. Glotfelter, J. Cortés, and M. Egerstedt, "A nonsmooth approach to controller synthesis for boolean specifications," *IEEE Transactions on Automatic Control*, vol. 66, no. 11, pp. 5160–5174, 2020.
- [24] R. W. Brockett, "Nonlinear systems and differential geometry," *Proceedings of the IEEE*, vol. 64, no. 1, pp. 61–72, 2005.
- [25] F. Bullo and A. D. Lewis, Geometric control of mechanical systems: modeling, analysis, and design for simple mechanical control systems. Springer, 2019, vol. 49.
- [26] R. Abraham, J. E. Marsden, and T. Ratiu, Manifolds, Tensor Analysis, and Applications. Springer Science & Business Media, 2012, vol. 75.
- [27] E. A. Coddington, N. Levinson, and T. Teichmann, "Theory of ordinary differential equations," 1956.
- [28] H. K. Khalil, Nonlinear Systems, 3rd ed. Upper Saddle River, NJ: Prentice Hall, 2002.
- [29] G. K. Batchelor, An introduction to fluid dynamics. Cambridge university press, 2000.
- [30] F. H. Clarke, "Generalized gradients and applications," Transactions of the American Mathematical Society, vol. 205, pp. 247–262, 1975.
- [31] F. H. Clarke, Y. S. Ledyaev, R. J. Stern, and R. Wolenski, Nonsmooth analysis and control theory. Springer, 1998.
- [32] F. H. Clarke, Optimization and nonsmooth analysis. SIAM, 1990.
- [33] L. Ambrosio, N. Gigli, and G. Savaré, Gradient flows: in metric spaces and in the space of probability measures. Springer, 2005.
- [34] S. P. Boyd and L. Vandenberghe, Convex optimization. Cambridge university press, 2004.
- [35] F. Albertini and E. D. Sontag, "Continuous control-lyapunov functions for asymptotically controllable time-varying systems," *International Journal of Control*, vol. 72, no. 18, pp. 1630–1641, 1999.
- [36] G. Notomista and M. Egerstedt, "Persistification of robotic tasks," *IEEE Transactions on Control Systems Technology*, vol. 29, no. 2, pp. 756–767, 2020.
- [37] X. Xu, "Constrained control of input-output linearizable systems using control sharing barrier functions," *Automatica*, vol. 87, pp. 195–201, 2018.
- [38] L. Lindemann and D. V. Dimarogonas, "Control barrier functions for signal temporal logic tasks," *IEEE control systems letters*, vol. 3, no. 1, pp. 96–101, 2018.
- [39] R. Lin and M. Egerstedt, ""Hierarchy of needs" for robots: Control synthesis for compositions of hierarchical, complex objectives," in 2025 IEEE International Conference on Robotics and Automation (ICRA). IEEE, 2025, pp. 7682–7688.
- [40] E. Sontag and H. J. Sussmann, "Nonsmooth control-lyapunov functions," in *Proceedings of 1995 34th IEEE conference on decision and control*, vol. 3. IEEE, 1995, pp. 2799–2805.
- [41] L. Wang, A. D. Ames, and M. Egerstedt, "Safety barrier certificates for collisions-free multirobot systems," *IEEE Transactions on Robotics*, vol. 33, no. 3, pp. 661–674, 2017.

- [42] S. Wilson, P. Glotfelter, L. Wang, S. Mayya, G. Notomista, M. Mote, and M. Egerstedt, "The robotarium: Globally impactful opportunities, challenges, and lessons learned in remote-access, distributed control of multirobot systems," *IEEE Control Systems Magazine*, vol. 40, no. 1, pp. 26–44, 2020.
- [43] R. Olfati-Saber, "Near-identity diffeomorphisms and exponential e-tracking and 6-stabilization of first-order nonholonomic SE(2) vehicles," Proceeding of the 2002 ACC, 2002.
- [44] S. Lloyd, "Least squares quantization in pcm," IEEE Transactions on Information Theory, vol. 28, no. 2, pp. 129–137, 1982.
- [45] J. Cortés, S. Martinez, T. Karatas, and F. Bullo, "Coverage control for mobile sensing networks: Variations on a theme," in *Mediterranean Conference on Control and Automation*. Lisbon, Portugal Lisbon, Portugal, 2002, pp. 9–13.